Influences of Different Implant Material Combinations on the Stress Distribution of the Foot Following Total Ankle Replacement: a Finite Element Analysis

Jian Yu
Huashan Hospital
Dahang Zhao
Ruijin Hospital, Shanghai Jiaotong University
Wen-Ming Chen
Fudan University
Pengfei Chu
Fudan University
Shuo Wang
Fudan University
Chao Zhang
Huashan Hospital
Jiazhang Huang
Huashan Hospital
Xu Wang
Huashan Hospital
Xin Ma (xin_ma@foxmail.com)
Huashan Hospital

Research Article

Keywords: Computational modeling, Finite element method, Implant design, Total ankle arthroplasty, Total ankle replacement

Posted Date: May 14th, 2021

DOI: https://doi.org/10.21203/rs.3.rs-497504/v1

Abstract

Background

A proper combination of implant materials for Total Ankle Replacement (TAR) may reduce stress at the implant and the foot. This study aimed to investigate the biomechanical influences for different implant material combinations using the finite element (FE) method.

Methods

A validated foot model was modified to simulate TAR with the INBONE II ankle system at the second peak ground reaction force. Six types of materials were used (Ceramic, cobalt–chromium–molybdenum alloy (CoCrMo), Titanium alloy (Ti6Al4V), carbon-fiber-reinforced Polyether-ether-ketone (CFR-PEEK), Polyether-ether-ketone (PEEK), and used ultra-high molecular weight polyethylene (UHMWPE)).

Results

The von Mises stress at the bearing articular surface decreased with implant stiffness. The combination of CFR-PEEK on UHMWPE presented the lowest stress of 14.82 MPa. A low implant stiffness of the talar component, rather than the bearing, relieved the stress at the resected surface of the talus.

Conclusions

Soft implant material provided a stress reduction at the bearing and adjacent bones. CFR-PEEK seemed to be a good alternative to implant metal components.

Introduction

Total ankle replacement (TAR) has become an essential and effective procedure for end-stage ankle arthritis [1]. The early and midterm clinical results of new-generation ankle implants appear promising [2, 3]. However, the long-term implant survivor rate is not comparable to that of total knee arthroplasty (TKA) or total hip arthroplasty (THA) [4-7]. The mechanism behind that is still unclear. The primary principle of TAR is to replace damaged ankle with artificial implants, therefore to alleviate pain and restore ankle function. After TAR, all forces are disseminated by the implant system across the articulating surfaces to the rest of the bones. The ankle joint typically experiences a higher joint force than the knee and hip joint during the gait, which can reach as much as 5-7 times of body weight [8, 9]. Replaced implant components alter the natural geometry and biomechanical characteristics of the ankle. Nevertheless, little is known about the biomechanics of the implant and the foot following TAR. Concentrated stress at the implant components or the adjacent bones may lead to accumulated damages to the implant articular surface or bony structure, thus wearing off the bearing component or causing cracks on bones, which

may result in a series of biomechanical complications, such as polyethylene failure, implant loosening, implant migration, and bone fracture. The mechanical properties of the implant system play a crucial role in avoiding local excessive bone stress [10-12]. A proper combination of implant materials may better reduce peak stress at the implant and the foot. Metal, ceramic, and polymer have been widely used as implant materials due to their high mechanical strength and biocompatibility [13-17]. Most existing total ankle implants have used ultra-high molecular weight polyethylene (UHMWPE) as bearing material and metal (cobalt–chromium–molybdenum alloy (Co-Cr-Mo) or Titanium alloy (Ti6Al4V)) as the material of tibial or talar components. Only one TAR system chose to use ceramic as tibial and talar component material (TNK ankle, Kyocera, Kyoto, Japan), which has been used in Japan for more than 30 years. The early clinical result is promising [18], but the long-term outcome is lacking. Polyether-ether-ketone (PEEK) and carbon-fiber-reinforced Polyether-ether-ketone (CFR-PEEK) have been used in joint replacement as a potential alternative to both the metal and bearing components [19-21]. PEEK materials have shown excellent strength, fatigue resistance, and their elastic moduli are lower than metal and ceramic, which should avoid metal ion release and stress shielding. However, the effect of different materials for TAR components on the biomechanics of the implant and bones have not been thoroughly investigated. Due to the difficulties in measuring the stress distributions on the implant and the foot bones, finite element (FE) simulation had been widely used for the pre-clinical biomechanical evaluation of orthopedic implants and scientific exploration for implant design. Only a few FE studies had investigated the stress characteristics at the implant articular surfaces: Espinosa et al. [22] constructed FE models of two TAR implants (MOBILITY and AGILITY) and found that misalignment of implant components induced high contact pressure. Ozen et al. [23] first developed a geometry accurate FE model of the whole foot and ankle implanted with Bueshel Pappas Total Ankle System at a balance standing position. More recently, Wang et al. [24, 25] also use a comprehensive FE foot model to compare the biomechanical difference of intact foot, foot with STAR ankle system, and foot after ankle arthrodesis. The present work aimed to (1) conduct a FE analysis of the foot model implanted with an ankle system and tested the prosthesis under maximum load in a realistic gait cycle; (2) investigate the biomechanical impact of different implant materials on the stress distribution at the implant articular surface and the adjacent bone.

Method

FE modeling of the foot and implant constructs

A previously validated three-dimensional FE model [26, 27] was modified to investigate the impact of different implant material combinations on the stress distribution of the implant and the foot after TAR. The foot model included thirty bones and enveloped soft tissue. All bones were connected by 134 major ligaments and a plantar fascia. The ligaments were represented by spring elements with a ‘no compression’ option. The 3D geometries of the plantar fascia and Achilles tendon were constructed. The other five muscle tendons, namely tibialis posterior (TIBP), flexor hallucis longus (FHL), flexor

digitorum longus (FDL), peroneus brevis (PB), and peroneus longus (PL), were also incorporated into the model using bar elements, at their corresponding anatomical attachment sites. Articular surfaces were modeled in the foot, with surface-to-surface contact elements.

The plantar soft tissue was modeled by an incompressible Ogden hyperelastic material [26]. The strain energy function U of the first-order Ogden model was defined by:

$$U = \frac{2\mu}{\alpha^2}(\lambda_1^\alpha + \lambda_2^\alpha + \lambda_3^\alpha - 3)$$

The material constants μ and α were determined by a previous in-vitro study [28] and equaled 3.75×10^{-2} MPa, and 5.5, respectively. Isotropic linear elastic material properties were assigned to the bones [29], ligaments [9], cartilages [30], plantar fascia[31], Achilles tendon [26, 32] and flexor tendon [33]. The details of the material parameters used in the foot model were given in **Table 1**. All 3-D structural components of the model were meshed by tetrahedral elements. A maximum edge length of 2.3 mm was determined by previous mesh convergence analysis and used in the current model.

Table 1 Material property and element type of the foot model

	Elastic modulus (MPa)	Poisson ratio	Cross-sectional area (mm2)	Element type
Bone	7300	0.3	-	4-node tet
Cartilage	1.01	0.4	-	4-node tet
Ligament	260	0.4	18.4	Spring
Plantar Fascia	350	0.4	-	4-node tet
Achilles tendon	816	0.3	-	4-node tet
Flexor tendon	450	0.3	12.5	Connector
Plantar soft tissue	1st Ogden incompressive hyperelastic model =0.0375 MPa, =5.5			4-node tet
Ground	Rigid			8-node hex

TAR implant modeling and implantation

In this study, we chose to replace a FE foot model with the INBONE II Total Ankle System (Wright Medical Technology, Inc., Memphis, TN, US) (see **Fig. 1**), the only ankle implant system currently used in China. It has a medullar segmented stem, assembled with a tibial tray, and a symmetric fixed bearing with full conformity to the talus component [34]. To the best of the authors' knowledge, no studies have previously investigated the biomechanical performance of this ankle system.

To match the shape of the current foot model, we chose and reverse engineered a size two long tibial component, a size two polyethylene insert with 6 mm thickness, and a size two talar component of the implant system. The materials of the tibial component, bearing, and talar component were Ti6Al4V, UHMWPE, and CrCoMo, respectively. Tibia and talus were resected with the protection of medial malleolus, and this ankle system was implanted following its operative guideline [35] from the manufacturer. The implantation procedure was guided and checked by two senior foot and ankle surgeons (XM and XW). The mesh size of the implant on contact biomechanics was determined by mesh convergence test (Supplementary **Table S1**). 1 mm mesh size at the articular surface, and 1.5 mm at the rest of the implant were chosen for model accuracy. UHMWPE was

modeled as an isotropic elastic-plastic material [36] with a yield stress of 10.86 MPa and a Poisson's ratio of 0.46. The stress-strain curve of the UHMWPE was presented in **Fig. 2**. The rest of the implant materials were modeled as isotropic elastic materials [10, 37, 38], and their mechanical properties were listed in **Table 2.** In this study, four types of materials were used to model tibial and talar components (Ceramic, Co-Cr-Mo, Ti6Al4V, and CFR-PEEK) while three types of materials were used to model bearing insert (CFR-PEEK, PEEK, and UHMWPE).

Table 2 Material property of the INBONE II Total Ankle System

Implant Material	Elastic modulus (MPa)	Poison ratio (ν)
Ceramic	350,000	0.26
Co-Cr-Mo	210,000	0.3
Ti6Al4V	114,000	0.342
CFR-PEEK	18,000	0.4
PEEK	4,100	0.36
UHMWPE	Stress-strain relationship [36]	0.46

Loading and boundary condition

Frictional contact interaction among the plantar surface and the ground was defined using a coefficient of friction (COF) of 0.5 [26]. The interaction between bone and implant was defined as a tie condition to simulate in-bone growth effects. The tibial tray and bearing were tied since its fix-bearing design. The bearing and talus interface was defined as frictionless [23].

We analyzed the biomechanical characteristics of the TAR implant at a time during the gait cycle when the ankle force reached a peak, namely the second peak of the ground reaction forces (GRF) associated with walking. A rigid plate under the foot was used to model the ground support. The ground was constrained to allow movement in a vertical direction only. The loading condition has previously been established in our foot FE model [26, 27]. In brief, a targeted maximum vertical GRF (623.1 N for the subject with a bodyweight of 60 kg) was generated solely by contracting plantar flexors corresponding to the push-off phase in gait. The obtained convergent solution of the muscle forces that maintain the second

metatarsal shaft orientation was 1620 N of GS complex, 267 N of the TIBP muscle, 130 N of the FHL muscle, 81 N of the FDL muscle, 91N of the PB muscle, and 193N of the PL muscle. Muscle forces of major plantar flexors were applied via the tendons attached. To only investigate the impact of implantation and implant material, we assumed all models shared the same as the boundary and loading conditions. The complete model was illustrated in **Fig. 3**.

Data Analysis

All FE models were solved in ABAQUS (Simulia Corp., Providence, RI, USA). The von Mises stress distribution on each bone, plantar surface pressure, von Mises stress distribution at the articular surface, and the resected surface of the talus were evaluated for each material combination.

Results

The plantar pressure distribution and von Mises stress distribution of the implant articular surface and the foot were given in **Fig. 4**. It can be seen that at the second peak of the GRF, plantar pressure concentrates at the forefoot and the plantar surface of the first toe **(Fig. 4b)**. The peak plantar pressure of the INBONE II implanted foot (Implant material: Ti6Al4V for tibial component, UHMWPE for the bearing, and CrCoMo for talar component) was 0.589 MPa, which was similar to that of the foot replaced with STAR total ankle system (0.605 MPa) [24]. The lateral force at the bearing was predicted to be higher than the medial force **(Fig. 4d)**, which was in good agreement with the simulation results of a musculoskeletal modeling study [39]. The total ankle force was 3463.18N, which was 5.89 times body weight (BW). Such an outcome was similar to the predicted total ankle reaction force of this ankle system, which ranged from 6.25 to 6.85 BW from the previous literature [39].

A sensitivity analysis of the effect of material properties of tibial components on the peak von Mises stress (see Supplementary **Table S2**) showed that for a given bearing material, the maximum difference for four materials of tibial component was less than 2.5%, indicating that the stiffness variation of the tibial component had a negligible impact on the stress at the bearing articular surface.

Comparison of von Mises stress distribution at the articular surface of the implant with the different material combinations.

Fig. 5 presented the stress distribution at the implant bearing surface with different material properties, specifically focusing on the material combination of the bearing and talar component. **Table 3** listed the peak von Mises stress of each material combination. Both **Fig. 5** and **Table 3** showed a general trend that peak stress decreased when the stiffness of implant material decreased. The combination of CFR-PEEK as the material of tibial and talar components and UHMWPE as the material of the bearing presented the lowest stress of 14.82 MPa. The maximum stress reduction of changing from CFR-PEEK to UHMWPE was 72.77%. The peak stress of the INBONE II implant system with the real material property (14.87 MPa) closely matched the minimum stress value.

Table 3 Peak von Mises stress at the articular surface of the implant with different material combinations

Peak von Mises stress		The material of Tibial and Talar components				Maximum difference
		Ceramic	CrCoMo	Ti6Al4V	CFR-PEEK	
Bearing Material	CFR-PEEK	51.26	49.39	47.06	36.86	28.09%
	PEEK	29.83	29.41	28.84	27.26	8.62%
	UHMWPE	14.96	14.92	14.86	14.82	0.94%
Maximum difference		72.77%	69.79%	68.43%	59.79%	

Comparison of von Mises stress distribution at the resected surface of the talus with the different material combinations.

The predicted results of the stress distribution and peak stress value at the resected surface of the talus for different implant material combinations showed that as the stiffness

of tibial and talar components decreased, the peak stress was slightly reduced (**Table 4**) and stress distributed more uniformly **(Fig. 6)**. The maximum stress reduction of changing from ceramic to CFR-PEEK was about 8.81%. However, the peak stress was insensitive to bearing stiffnesses (the maximum difference of peak stress value was less than 5%).

Table 4 Peak von Mises stress at the resected surface of the talus for different implant material combinations

Peak von Mises stress		The material of Tibial and Talar components				Maximum difference
		Ceramic	CrCoMo	Ti6Al4V	CFR-PEEK	
Bearing Material	CFR-PEEK	9.068	9.070	9.028	8.312	7.312%
	PEEK	9.068	9.051	9.000	8.373	7.66%
	UHMWPE	9.415	9.271	9.101	8.586	8.81%
Maximum difference		3.69%	2.37%	1.11%	3.19%	

Discussion

The present computational model was developed to investigate the biomechanical influences of six implant materials on the implant bearing and adjacent bone. What distinguished our model from previous FE studies was that (a) it determined the stress characteristics of the implant and the foot with the consideration of the whole structure of foot and ankle while accounting for the impact of twelve implant material combinations and (b) the detailed geometry of the INBONE II total ankle implant was included, which has not been tested in the previous studies. Kerschhofer et al. [37] tested PEEK and its composites on Wright State University (WSU) TAR devices. CFR-PEEK/UHMWPE material model exhibited lower contact stress and wear rate compared with Ti6Al4V/UHMWPE material model. Through a tibial bone-implant construct of the STAR ankle system, Mondal et al. [10] revealed implant materials had less impact on tibia bone strain and micromotion. And wear depth was reduced when the ceramic and CFR-PEEK material combination was used. However, the two studies mentioned above only considered partial models of the foot-implant constructs; thus, the stress characteristics were largely ignored.

Our results revealed that stress distribution at the articular surface of the implant bearing exhibited a higher sensitivity to the material of bearing, rather than the material of the tibial or talar component. Bearing with UHMWPE showed the lowest contact stress, which may be one reason why UHMWPE is commonly used as the bearing material. The peak von Mises stress of the implant with CFR-PEEK as the material of tibial and talar components and UHMWPE as the material of the bearing at the second peak of the GRF is 14.82 MPa, which is below the yield stress of UHMWPE (19–21 MPa) [40]. The metal-on-metal implant configuration is not considered in this study since no such arrangement has been used in existing ankle replacement implant systems, and concerns have been raised about its use in hip and knee arthroplasty by researchers [41] and the FDA of United States [42].

In addition, our results showed that the material of the talar component made a small impact on the stress at the resected surface of the talus, which was insensitive to the variation of implant bearing material stiffness. High stress concentrated at adjacent bone may cause pain or implant subsidence. The talar component with a smaller material stiffness can smooth the stress change across the resected surface of the talus, informing CFR-PEEK seems to be a good alternative to metal components biomechanically. However, future studies should perform more comprehensive evaluations of the PEEK composite before its application to clinical practice.

One major limitation of the study is that several assumptions were made for simplification, such as no separation of cortical and trabecular bone, no consideration of the creep property of the UHMWPE and the bone remodeling process. The boundary and loading conditions were also assumed to be the same as the intact foot. Future studies should increase the complexity, thus to better mimic the property of a real prosthetic foot. What's more, the current foot model was developed from the CT images of one healthy volunteer and replaced by one model. Future studies should consider using the radiological data of more patients with the surgical implication of total ankle replacement of this ankle system to provide substantial clinical importance for the predicted results.

Conclusion

Soft implant material could provide a stress reduction at both the bearing articular surface and the adjacent bones. CFR-PEEK as the material of tibial and talar component and UHMWPE as the bearing material exhibited the lowest peak stress value at the implant bearing and adjacent bone, thus seemed to be a promising material combination from the biomechanical perspective. Such results provided insight into the biomechanics of the TAR procedure and material selection of implant components. The FE foot model with the INBONE II ankle system can be utilized for further biomechanical investigations of TAR and implant optimization, eventually benefit patients who need TAR in the clinical practice.

Declarations

Ethics approval and consent to participate

Not applicable

Consent for publication

Not applicable

Availability of data and materials

The datasets used and analyzed during the current study are available from the corresponding author on reasonable request.

Competing interests

The authors declare that they have no competing interests.

Funding

This project was supported by the Scientific and Technological Innovation of Shanghai Science and Technology Committee (Grant No. 18441902200), Natural Science Foundation of Shanghai (Grant No. 19ZR1407400), Clinical Research Plan of SHDC (Grant No. SHDC2020CR3071B), and National Natural Science Foundation of China (Grant No. 82072388 and 81702109).

Authors' contributions

J.Y. and D.Z. contributed equally to this study. J.Y. and D.Z. performed the finite element analysis, drafted the manuscript and designed the figures. D.Z., W.C. and P.C. aided in interpreting the results and worked on the manuscript. S.W., C.Z. and J.H. performed the measurements, X.M. and X.W. were involved in planning and supervised the work. All authors discussed the results and commented on the manuscript.

Acknowledgments

None

Author details

a Department of Orthopedics, Huashan Hospital, Fudan University, Shanghai, China. b Department of Orthopedics, Ruijin Hospital, Shanghai Jiaotong University, Shanghai, China. c Academy for Engineering and Technology, Fudan University, Shanghai, China

References

1. Raikin SM, Rasouli MR, Espandar R, Maltenfort MG. **Trends in Treatment of Advanced Ankle Arthropathy by Total Ankle Replacement or Ankle Fusion**. *Foot & Ankle International* 2014, **35**(3):216–224.

2. Gougoulias N, Khanna A, Maffulli N. **How successful are current ankle replacements?: a systematic review of the literature**. *CLINICAL ORTHOPAEDICS AND RELATED RESEARCH* 2010, **468**(1):199–208.
3. Daniels TR, Younger ASE, Penner M, Wing K, Dryden PJ, Wong H, Glazebrook M. **Intermediate-term results of total ankle replacement and ankle arthrodesis: a COFAS multicenter study**. *The Journal of bone and joint surgery American volume* 2014, **96**(2):135–142.
4. Lee G-W, Wang S-H, Lee K-B. **Comparison of Intermediate to Long-Term Outcomes of Total Ankle Arthroplasty in Ankles with Preoperative Varus, Valgus, and Neutral Alignment**. *The Journal of bone and joint surgery American volume* 2018, **100**(10):835–842.
5. Clough T, Bodo K, Majeed H, Davenport J, Karski M. **Survivorship and long-term outcome of a consecutive series of 200 Scandinavian Total Ankle Replacement (STAR) implants**. *The Bone & Joint Journal* 2019, **101-B**(1):47–54.
6. Mäkelä KT, Matilainen M, Pulkkinen P, Fenstad AM, Havelin L, Engesaeter L, Furnes O, Pedersen AB, Overgaard S, Kärrholm J *et al*. **Failure rate of cemented and uncemented total hip replacements: register study of combined Nordic database of four nations**. *BMJ: British Medical Journal* 2014, **348**:f7592.
7. Victor J, Ghijselings S, Tajdar F, Van Damme G, Deprez P, Arnout N, Van Der Straeten C. **Total knee arthroplasty at 15–17 years: Does implant design affect outcome?** *International Orthopaedics* 2014, **38**(2):235–241.
8. Bell CJ, Fisher J. **Simulation of polyethylene wear in ankle joint prostheses**. *J Biomed Mater Res B Appl Biomater* 2007, **81**(1):162–167.
9. Siegler S, Block J. **The Mechanical Characteristics of the Collateral Ligaments of the Human Ankle Joint**. *Foot and Ankle* 1988, **8**(5):234–242.
10. Mondal S, Ghosh R. **Effects of implant orientation and implant material on tibia bone strain, implant-bone micromotion, contact pressure, and wear depth due to total ankle replacement**. *Proceedings of the Institution of Mechanical Engineers Part H, Journal of engineering in medicine* 2019, **233**(3):318–331.
11. Chang B, Brown PR, Sieber A, Valdevit A, Tateno K, Kostuik JP. **Evaluation of the biological response of wear debris**. *The Spine Journal* 2004, **4**(6):S239-S244.
12. Figgie MP, Wright TM, Drinkwater D, Bioengineering Working G. **What design and material factors impact the wear and corrosion performance in total elbow arthroplasties?** *Clinical orthopaedics and related research* 2014, **472**(12):3770–3776.
13. Manam NS, Harun WSW, Shri DNA, Ghani SAC, Kurniawan T, Ismail MH, Ibrahim MHI. **Study of corrosion in biocompatible metals for implants: A review**. *Journal of Alloys and Compounds* 2017, **701**:698–715.
14. Lorusso F, Noumbissi S, Francesco I, Rapone B, Khater AGA, Scarano A. **Scientific Trends in Clinical Research on Zirconia Dental Implants: A Bibliometric Review**. *Materials* 2020, **13**(23):5534.
15. Scarano A, Lorusso F, Inchingolo F, Postiglione F, Petrini M. **The Effects of Erbium-Doped Yttrium Aluminum Garnet Laser (Er: YAG) Irradiation on Sandblasted and Acid-Etched (SLA) Titanium, an In**

Vitro Study. *Materials* 2020, **13**(18):4174.

16. Kurtz SM, Devine JN. **PEEK biomaterials in trauma, orthopedic, and spinal implants**. *Biomaterials* 2007, **28**(32):4845–4869.
17. Sandler J, Werner P, Shaffer MSP, Demchuk V, Altstädt V, Windle AH. **Carbon-nanofibre-reinforced poly(ether ether ketone) composites**. *Composites Part A: Applied Science and Manufacturing* 2002, **33**(8):1033–1039.
18. Kurokawa H, Taniguchi A, Morita S, Takakura Y, Tanaka Y. **Total ankle arthroplasty incorporating a total talar prosthesis**. *The Bone & Joint Journal* 2019, **101-B**(4):443–446.
19. Latif AMH, Mehats A, Elcocks M, Rushton N, Field RE, Jones E. **Pre-clinical studies to validate the MITCH PCR™ Cup: a flexible and anatomically shaped acetabular component with novel bearing characteristics**. *Journal of Materials Science: Materials in Medicine* 2008, **19**(4):1729–1736.
20. Rankin KE, Dickinson AS, Briscoe A, Browne M. **Does a PEEK Femoral TKA Implant Preserve Intact Femoral Surface Strains Compared With CoCr? A Preliminary Laboratory Study**. *Clinical Orthopaedics and Related Research* 2016, **474**(11):2405–2413.
21. Koh Y-G, Park K-M, Lee J-A, Nam J-H, Lee H-Y, Kang K-T. **Total knee arthroplasty application of polyetheretherketone and carbon-fiber-reinforced polyetheretherketone: A review**. *Materials Science and Engineering: C* 2019, **100**:70–81.
22. Espinosa N, Walti M, Favre P, Snedeker JG. **Misalignment of total ankle components can induce high joint contact pressures**. *The Journal of bone and joint surgery American volume* 2010, **92**(5):1179–1187.
23. Ozen M, Sayman O, Havitçioğlu H. **Modeling and stress analyses of a normal foot-ankle and a prosthetic foot-ankle complex**. *Acta of bioengineering and biomechanics / Wrocław University of Technology* 2013, **15**:19–27.
24. Wang Y, Li Z, Wong DW-C, Cheng C-K, Zhang M. **Finite element analysis of biomechanical effects of total ankle arthroplasty on the foot**. *Journal of Orthopaedic Translation* 2018, **12**:55–65.
25. Wang Y, Wong DW-C, Tan Q, Li Z, Zhang M. **Total ankle arthroplasty and ankle arthrodesis affect the biomechanics of the inner foot differently**. *Scientific reports* 2019, **9**(1):13334–13334.
26. Chen W-M, Park J, Park S-B, Shim VP-W, Lee T. **Role of gastrocnemius–soleus muscle in forefoot force transmission at heel rise — A 3D finite element analysis**. *Journal of Biomechanics* 2012, **45**(10):1783–1789.
27. Chen W-M, Lee S-J, Lee PVS. **Plantar pressure relief under the metatarsal heads – Therapeutic insole design using three-dimensional finite element model of the foot**. *Journal of Biomechanics* 2015, **48**(4):659–665.
28. Chen W-M, Phyau-Wui Shim V, Park S-B, Lee T. **An instrumented tissue tester for measuring soft tissue property under the metatarsal heads in relation to metatarsophalangeal joint angle**. *Journal of Biomechanics* 2011, **44**(9):1801–1804.
29. Cheung JT-M, Zhang M, Leung AK-L, Fan Y-B. **Three-dimensional finite element analysis of the foot during standing—a material sensitivity study**. *Journal of Biomechanics* 2005, **38**(5):1045–1054.

30. Athanasiou KA, Liu LA, Lavery DR, Lanctot RC, Jr., Schenck RC, Jr.. **Biomechanical topography of human articular cartilage in the first metatarsophalangeal joint**. *Clinical Orthopaedics and Related Research* 1998, **348**(0009-921X (Print)):269–281.
31. Wright DC, Rennels DC. **A study of the elastic properties fo plantar fascia**. *jbjs* 1964, **46**(0021-9355 (Print)):482–492.
32. Wren TAL, Yerby SA, Beaupré GS, Carter DR. **Mechanical properties of the human achilles tendon**. *Clinical Biomechanics* 2001, **16**(3):245–251.
33. García-González A, Bayod J, Prados-Frutos JC, Losa-Iglesias M, Jules KT, de Bengoa-Vallejo RB, Doblaré M. **Finite-element simulation of flexor digitorum longus or flexor digitorum brevis tendon transfer for the treatment of claw toe deformity**. *Journal of Biomechanics* 2009, **42**(11):1697–1704.
34. Gross CE, Palanca AA, DeOrio JK. **Design Rationale for Total Ankle Arthroplasty Systems: An Update**. *J Am Acad Orthop Surg* 2018, **26**(10):353–359.
35. **INBONE II Total Ankle System SURGICAL TECHNIQUE**. www.wrightemedia.com/ProductFiles/Files/PDFs/016414_EN_HR_LE.pdf. Accessed 1 May 2021.
36. Miller MC, Smolinski P, Conti S, Galik K. **Stresses in polyethylene liners in a semiconstrained ankle prosthesis**. *J Biomech Eng* 2004, **126**(5):636–640.
37. Kerschhofer D, Gundapaneni D, Christof S, Goswami T. **Applicability of PEEK and its composites in total ankle replacement devices and wear rate predictions**. *Biomedical Physics and Engineering Express* 2016, **2**(6).
38. Manley MT, Ong KL, Kurtz SM.**The potential for bone loss in acetabular structures following THA**. *Clinical Orthopaedics and Related Research* 2006, **453**(453):246–253.
39. Zhang Y, Chen Z, Zhao H, Liang X, Sun C, Jin Z. **Musculoskeletal modeling of total ankle arthroplasty using force-dependent kinematics for predicting in vivo joint mechanics**. *Proceedings of the Institution of Mechanical Engineers, Part H: Journal of Engineering in Medicine* 2020, **234**(2):210–222.
40. **Standard Specification for Ultra-High-Molecular-Weight Polyethylene Powder and Fabricated Form for Surgical Implant**. https://www.astm.org/Standards/F648.htm. Accessed 1 May 2021.
41. J. DM, V. P, B. W, G. R. **Metal-on-metal hip surface replacement**. *The Bone & Joint Journal* 2014, **96-B**(11_Supple_A):17–21.
42. **Concerns about Metal-on-Metal Hip Implants**. https://www.fda.gov/medical-devices/metal-metal-hip-implants/concerns-about-metal-metal-hip-implants. Accessed 1 May 2021.

Figures

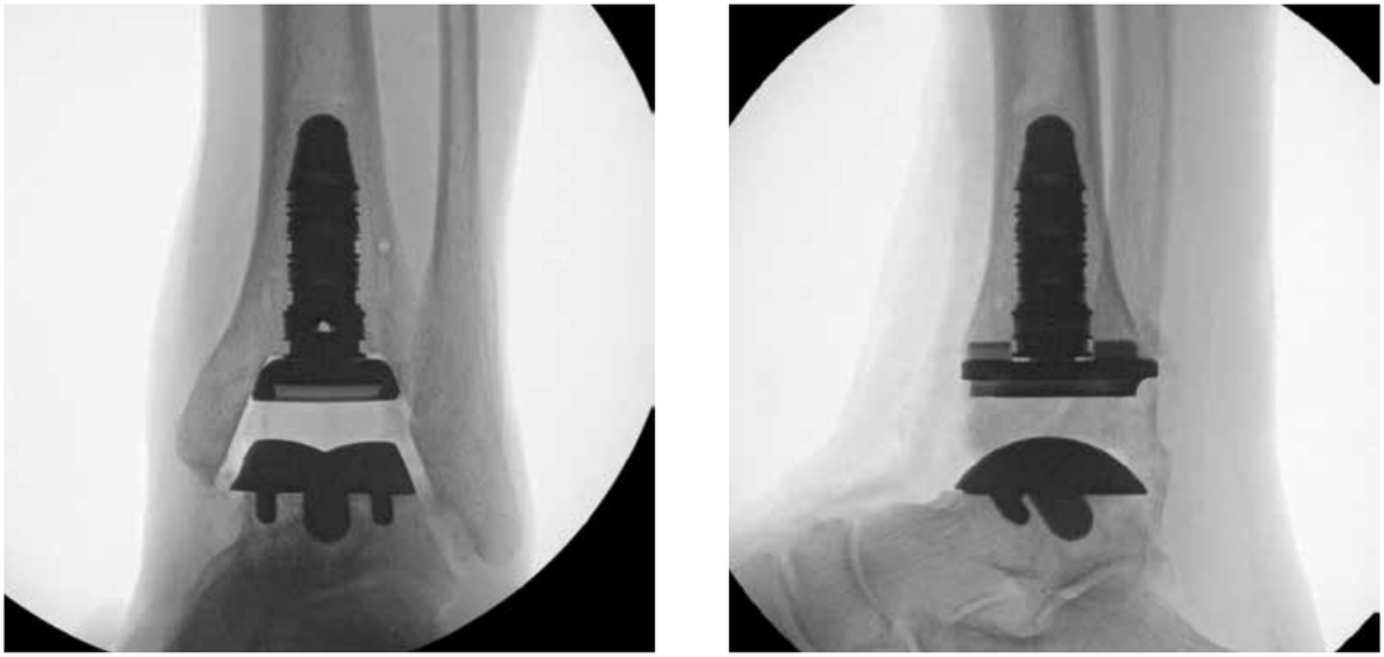

Figure 1

X-ray images of the INBONE II ankle system. Intra-operative anterior-posterior and lateral fluoroscopic images of the ankle with INBONE II Total Ankle System. (Image courtesy of Wright Medical Technology, Inc., Memphis, TN, US)

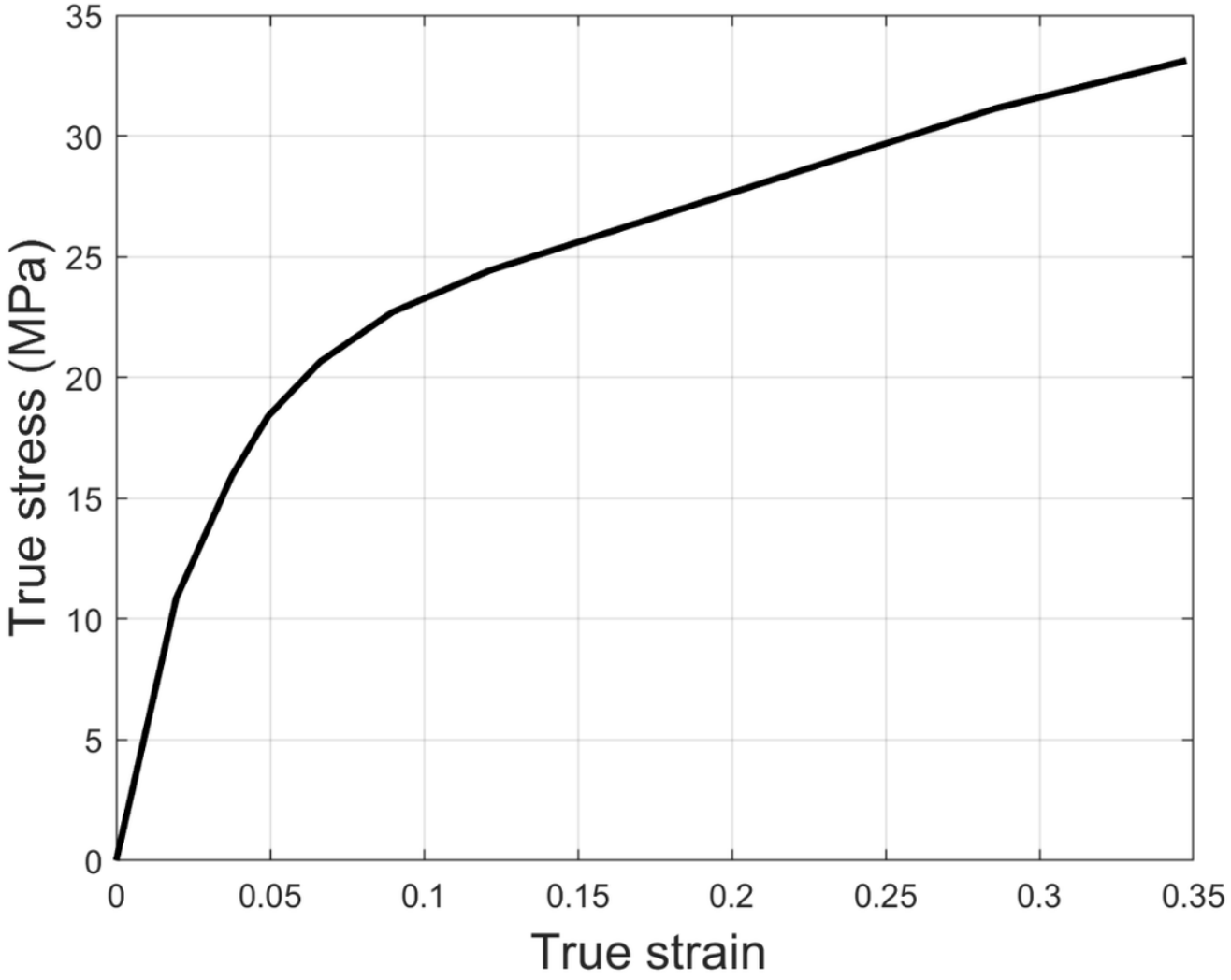

Figure 2

The stress-strain curve of the UHMWPE material [36]

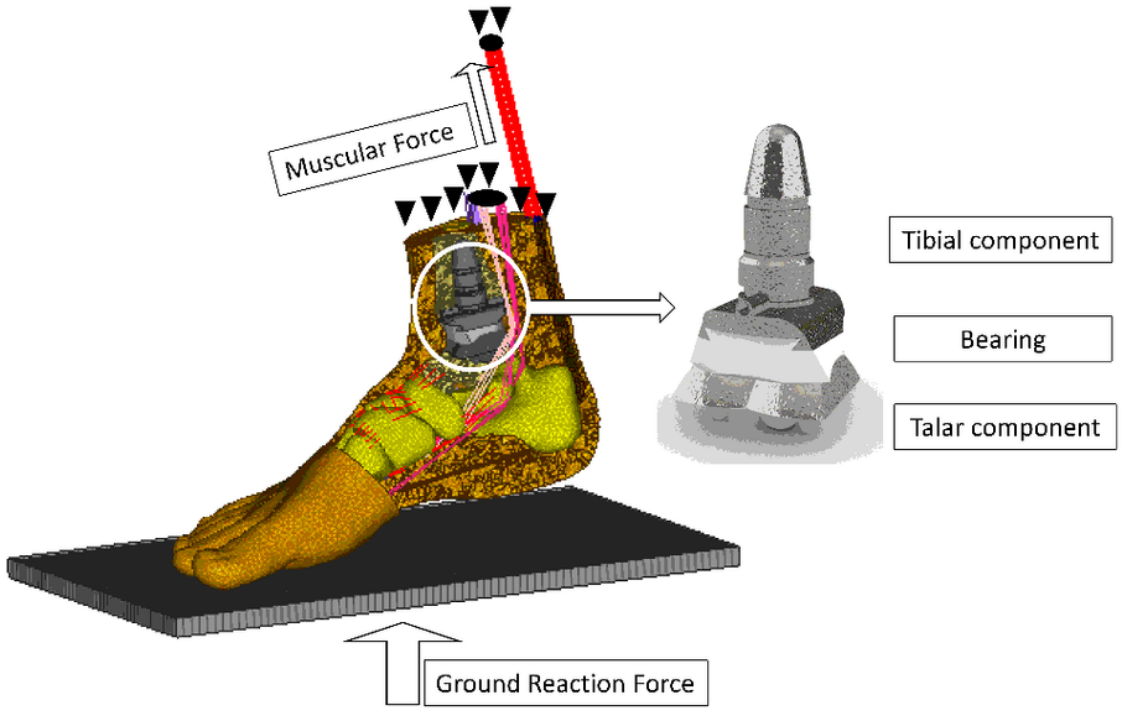

Figure 3

An illustration of the FE foot model implanted with INBONE II Total Ankle System (Tibial component size: size 2 long. Bearing size: size 2 polyethylene insert with 6 mm thickness. Talar component size: size 2)

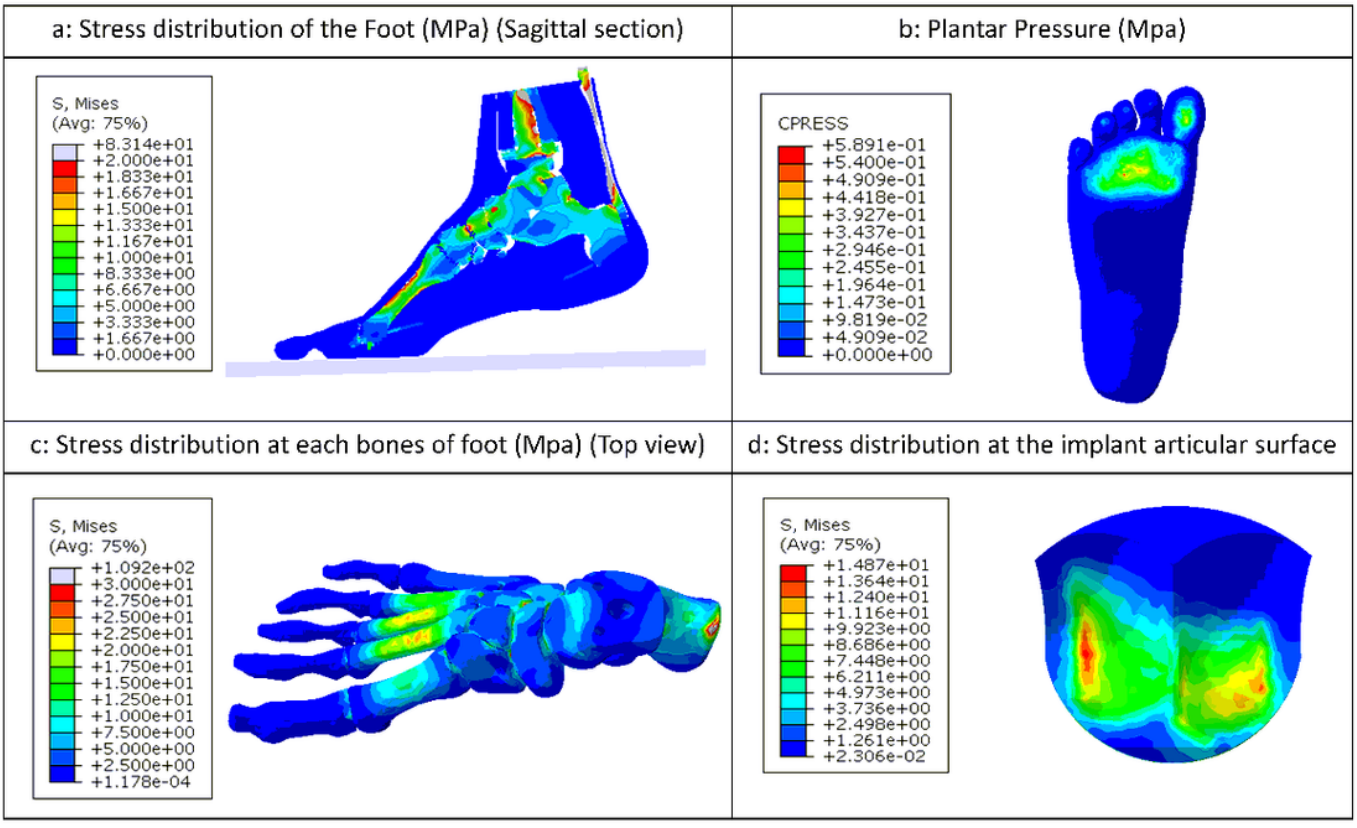

Figure 4

The plantar pressure distribution and von Mises stress across the foot of both the intact foot and implated foot (Implant material: Ti6Al4V as tibial component material, UHMWPE as bearing material and CrCoMo as talar component material)

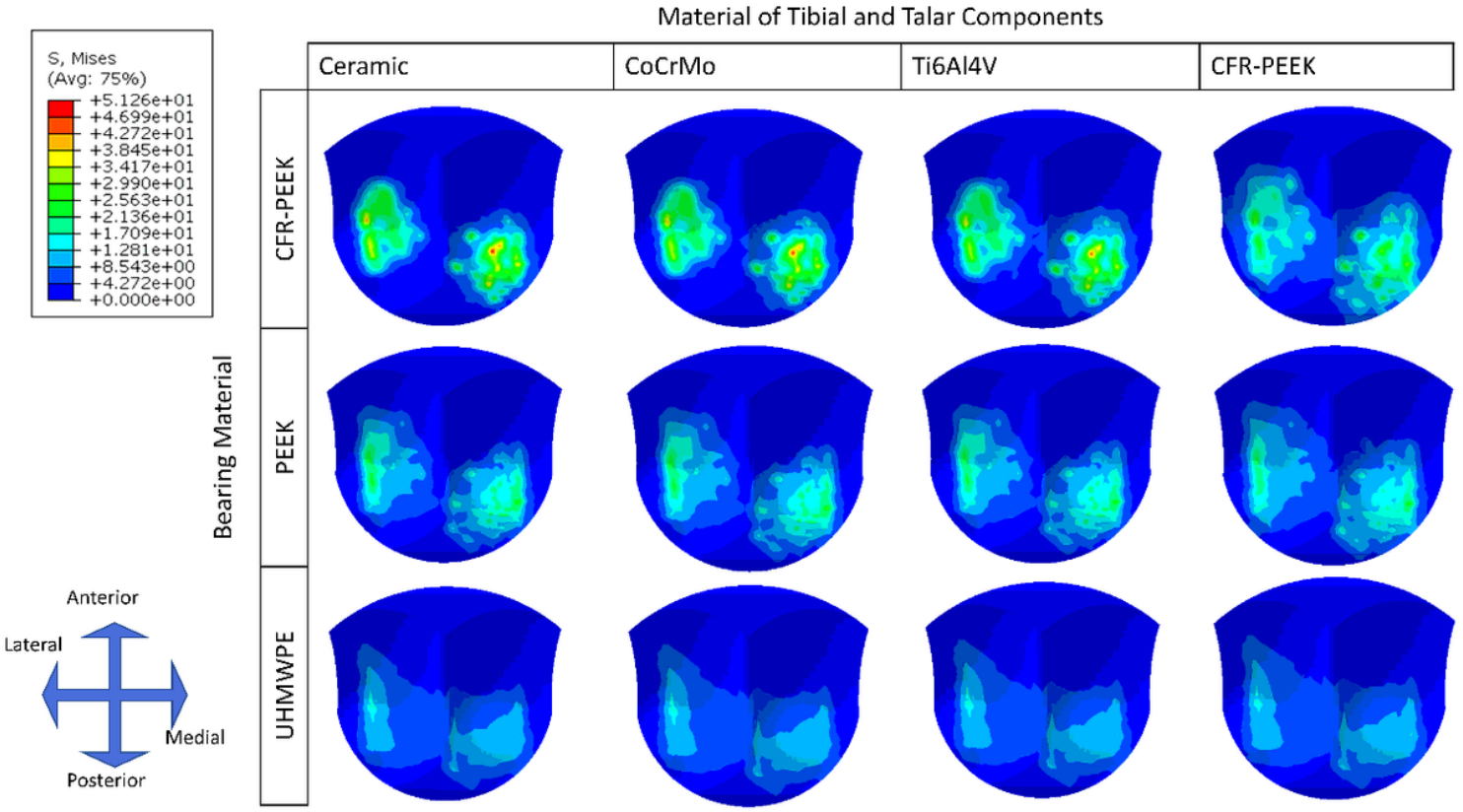

Figure 5

The von Mises stress distribution at the articular surface of the implant with different material combinations

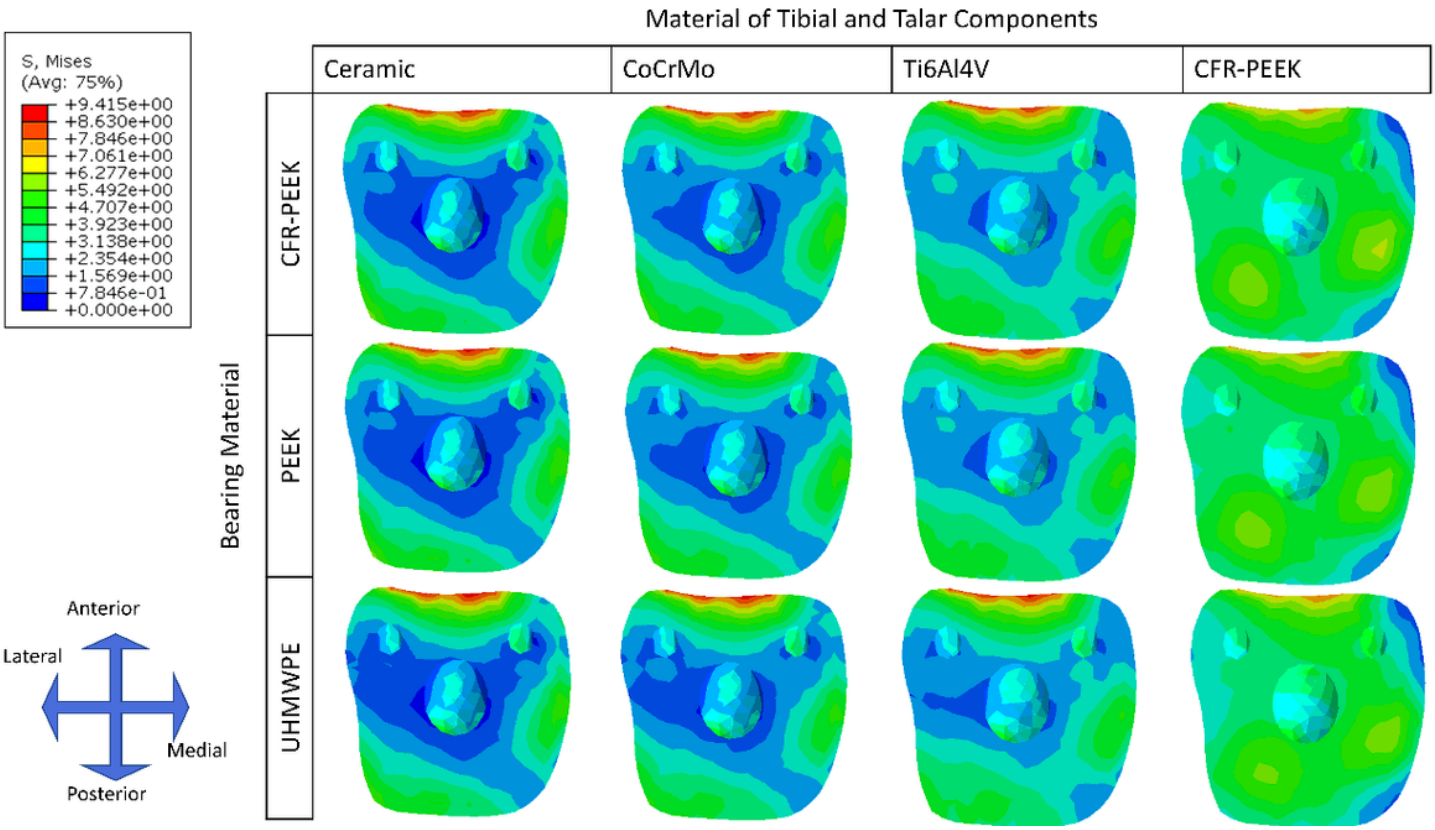

Figure 6

The von Mises stress distribution at the resected surface of the talus for different implant material combinations

Supplementary Files

This is a list of supplementary files associated with this preprint. Click to download.

- SupplementaryInformation.docx